Control of Molecular Structure in the Generation of Highly Luminescent Liquid Crystalline Perylenebisimide Derivatives: Synthesis, Liquid Crystalline and Photophysical Properties

B. Jancy and S. K. Asha*

Specialty Polymers, Chemical Sciences & Technology Division, Regional Research Laboratory (CSIR), Thiruvananthapuram 695019, Kerala, India

Received: June 23, 2006; In Final Form: July 15, 2006

We report here, for the first time, the role of the molecular design on the liquid crystalline and solid-state photoluminescent properties of soluble and thermally stable liquid crystalline perylenebisimide derivatives. A new series of perylenebisimides were designed and developed for this purpose by adopting the stoichiometry-control approach, and amine-, hydroxyl-, ester-, and amide-functionalized molecules were synthesized. Various types of spacers with different lengths (C_2 to C_{12}), types (linear, cyclohexyl, and tricyclodecane), and end-capped by phenyl or tridodecyloxy gallic units were introduced in the perylenebisimide core. The molecules were completely characterized by NMR, FT-IR, SEC, and MALDI-TOF mass techniques. Thermal analysis revealed that the perylenebisimide derivatives were thermotropic liquid crystalline, and threadlike nematic phases were observed under a polarizing light microscope. The spacer length and the rigidity of the spacers play a major role in the liquid crystalline properties of the materials. In phenyl systems, the C_6 chain with ester- and the C_{12} chain with amide-end-capped molecules showed a nematic phase, whereas the C_6 chain with an amide end cap and their cyclic and tricyclic counterparts did not show any LC property. The introduction of a tridodecyloxy gallic unit induced the LC property in C_{12} and the cyclohexyl system; however, it failed to do so in the tricyclodecane molecule. The absorption properties of the molecules were almost unchanged by the structural variation; however, the emission quantum yield in solution and photoluminescent (PL) intensity in the solid state were significantly different. Though the gallic unit induced liquid crystallinity in the perylenebisimide core, the quantum yield and PL intensity are 4−5 times less compared to those of the simple phenyl-capped liquid crystalline system. Among the various types of spacers, the tricyclodecane induced strong molecular aggregates via π-stacking, which in turn increased the rigidity of the entire perylenebisimide core, resulting in the absence of liquid crystallinity and low luminescence compared to their linear and cyclohexyl analogues. The molecular aggregates were very stable even at very dilute concentration and also at high temperatures. The aggregates disappeared immediately upon addition of trifluoroacetic acid, thus confirming the strong hydrogen bonding in the aggregated states. In a nutshell, the present report demonstrates the importance of molecular design for introducing liquid crystalline phases in perylenebisimides and also the development of novel highly luminescent n-type π-conjugated material for application in optoelectronics.

Introduction

Perylenebisimide derivatives represent an important class of n-type semiconductors exhibiting a relatively high electron affinity among large-band-gap materials. Perylenebisimide derivatives are inexpensive, readily available, robust compounds, and they are well-known chromophores combining high quantum yields of photoluminescence with excellent photochemical and thermal stability. They are of interest and are successfully used in colorful liquid crystal displays, as dye sensitizers in solar cells, in electrophotographic applications, and as molecular components of light-emitting diodes.[1−8] The development of perylenebisimide-based materials with high charge carrier mobility has improved the performance of OLEDs and solar cells. In this respect, liquid crystalline perylenebisimides are particularly useful since they possess the ability to self-organize spontaneously into highly ordered structures, and the liquid crystalline materials are known to exhibit better transport properties. However, there are only a few reports of perylene-based liquid crystalline materials in the literature.[9−20] In general, there are two approaches commonly adopted to induce liquid crystallinity in perylenebisimides: (i) introduction of suitable imide linkages by reaction of the peripheral bisanhydrides with aliphatic or aromatic amines, and (ii) the derivatization of the aromatic core via halogenation (bay substitution) and subsequently with suitable substitution reactions. Cormier et al. demonstrated the imide-derivative approach for linear and branched oligo(oxyethylene) chains and extensively studied their self-organization in thin films and also self-assembly at the air/water interfaces. Most of these perylenebisimide derivatives were monotropic and low-melting materials, which transformed into crystalline phases upon standing.[9,10] Frank Würthner and co-workers have introduced the bay substitution approach for columnar liquid crystalline perylenebisimides and diazadibenzoperylenes and investigated the aggregation and charge carrier properties.[19,20] One of the major limitations in the latter approach is that the planarity of the perylenebisimide is drastically affected by the bay substitution due to increased steric hindrance, which in turn affects the optical or electronic properties of this class of materials.[21−23] Liquid crystalline perylene derivatives based

* Corresponding Author. Fax: 0091-471-2491712. E-mail: ashask@csrrltrd.ren.nic.in.

10.1021/jp063943c CCC: $33.50
Published on Web 09/20/2006

SCHEME 1: Structures of Novel LC Perylenebisimides

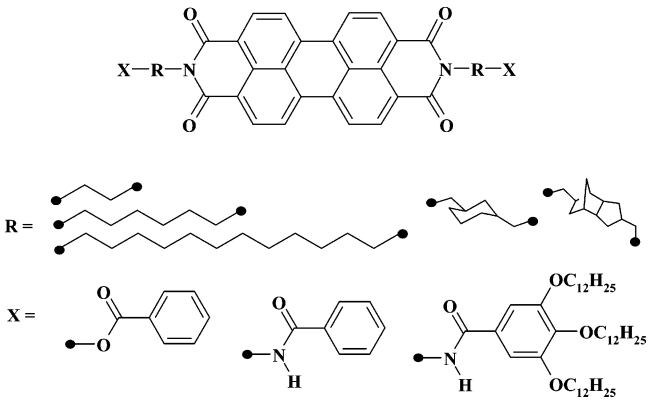

on triazoline-3,5-diones and ionic self-assembled cationic perylenedimide−surfactant complexes, and so forth, were also reported, and their liquid crystalline properties were investigated in detail.[14] Recently, there were reports of perylenebisimide−oligo(phenylenevinylene) donor−acceptor−donor triad systems, either connected directly or through a branched spacer segment where only the former showed liquid crystalline behavior.[24,25] Trialkoxy-substituted gallic acid derivatives end-capped at the imide linkages have also been shown to induce liquid crystallinity in the perylenebisimides.[17] Though the above-mentioned various independent approaches were successful in developing liquid crystalline perylenebisimides, most of them focused on specific issues of self-organization of aggregates. In general, there is a lack of a systematic effort to understand the structural requirement for introducing liquid crystalline (LC) phases in perylenebisimides and also the effect of LC phases on the luminescent properties. Additionally, most of the approaches were also limited to small molecular systems, and extending the concepts to processable polymers becomes almost impossible because of the tedious multistep synthesis and lack of reactive sites for further reactions. A new molecular design consisting of liquid crystalline perylenebisimide mesogens with reactive functional groups would be very attractive to address the above issue and also in the future development of highly ordered liquid crystalline, freely soluble, processable, and mechanically stable systems for optoelectronic devices based on perylenebisimides.

The present investigation emphasizes the design and development of novel, highly luminescent perylenebisimides with functional groups such as hydroxyl, amine, amide, and ester, which could be used in the long term as intermediates for many other macromolecular architectures. In addition to the liquid crystallinity, the approach is also focused on developing highly luminescent perylenebisimide derivatives, a property that is one of the most essential properties for application in optoelectronic devices. The present work also addresses fundamental questions regarding the structural requirement for introducing liquid crystalline phases in perylenebisimides; examples are the length, nature (linear or cyclic), and types of the chemical linkages (amide or ester) of the solubilizing pendants. The structures of the new perylene bisimides are given in Scheme 1.

The design strategy that was adopted in this series was to vary the length of the linear alkyl spacer (ethyl to dodecyl), vary the nature of the spacer segment (flexible or rigid) via linear alkyl chain or cycloaliphatic ring, as well as to vary the type of the functionality in the terminal, that is, hydroxyl, amine, ester, or amide. Two new cycloaliphatic diamines such as 1,3-cyclohexyl(bismethylamine) and 3,8-bis(aminomethyl)tricyclo-[5.2.1.0.(2,6)]decane (TCD-DA) and their linear counterparts with various lengths (C_2 to C_{12}) were chosen to study the effect of spacers that can introduce varying extents of rigidity. The rigidity of cycloaliphatic units is between that of flexible linear alkyl and rigid aromatic units. The cycloaliphatic spacers were thus chosen with the expectation that their introduction would bring in the optimum balance of rigidity and flexibility that is an essential requirement for inducing liquid crystallinity. The amine-functionalized perylenebisimides were prepared in a one-pot synthesis by stoichiometry control of the perylenebisanhydride with diamines. The structures of the molecules were confirmed by NMR, FT-IR, SEC, and MALDI-TOF techniques. Additionally, effort was also devoted to understanding the aggregation phenomena, electrochemical properties, and solid-state luminescence of the liquid crystalline perylenebisimide derivatives. In a nutshell, the present approach is aimed at understanding the molecular design requirement for introducing liquid crystalline phases in perylenebisimides to explore as futuristic n-type highly luminescent π-conjugated materials for application in ligh-emitting diodes and photovoltaic cells.

Experimental Section

Materials. Perylene-3,4,9,10-tetracarboxylicdianhydride (PTCDA), 1,3-cyclohexyl(bismethylamine) (CHBMA), 1,12-diaminododecane, 6-aminohexanol, *N*,*N*-dimethylacetamide (DMAc), *N*-methyl pyrrolidinone (NMP), 3,4,5-trihydroxy benzoic acid, 1-bromododecane, and Rhodamine-6G were purchased from Sigma Aldrich and used without further purification. 3,8-Bis-(aminomethyl)-tricyclo[5.2.1.0.(2,6)]decane (TCD-DA) was kindly supplied by Celanese Chemicals. Ethanolamine, zinc acetate, benzoyl chloride, and pyridine were purchased locally and purified using standard procedures.

Instrumentation and Characterization. ^{1}H NMR spectra were recorded using a 300-MHz Brucker NMR spectrophotometer in $CDCl_3$ or $CDCl_3$/TFA containing small amounts of TMS as an internal standard. The purity of the compounds was determined by a Shimadzu QP-2000 (GC/MS) Micromass Tof Spec 2E instrument using a nitrogen 337-nm laser (4-ns pulse).The matrix used was 2,5-dihydroxy benzoic acid dissolved in $CHCl_3$ which was spotted on the MALDI target and allowed to dry before introduction into the mass spectrometer. The purity of the oligomers was further analyzed by SEC in THF using polystyrene standards for the calibration. A Waters 510 pump connected through three series of styragel HR columns (HT-3, HT-4, and HT-5) and a Waters model 2487 dual wavelength UV−vis detector were used for analyzing the samples. The flow rate of the THF was maintained as 1 mL throughout the experiments, and the sample solutions at very dilute concentrations were filtered and injected for recording the GPC chromatograms at 30 °C. Infrared spectra were recorded using a Perkin-Elmer, Spectrum One FT-IR spectrophotometer in the range of 4000 to 400 cm^{-1}. Absorption spectra were recorded using a Perkin-Elmer Lambda 35 UV−vis spectrometer. The emission studies were performed by a SPEX Fluorolog F112X spectrofluorimeter. For recording solid-state photophysical properties, thin films were cast from chloroform solution onto a glass plate and allowed to dry for 24 h prior to measurements. The film thicknesses were varied by changing the concentration of the solution. The fluorescence quantum yields of the perylene derivatives were determined in $CHCl_3$ using Rhodamine-6G in water ($\phi = 0.95$) as the standard by exciting at 524 nm. The optical density at λ_{524} was maintained at 0.1 ± 0.05 to avoid reabsorption artifacts. Thermogravimetric analysis (TGA) was performed using a TGA-50 Shimadzu thermogravimetric analyzer. Samples were run from 40 to 700 °C with a heating rate of 10 °C/min under nitrogen. DSC

measurements were performed on a DSC−Perkin-Elmer Pyris 6 DSC instrument at a heating rate of 10 °C/min under a nitrogen atmosphere. Typically, 2−3 mg of samples was placed in an aluminum pan, sealed properly, and scanned from 10 to 280 °C. The instrument was calibrated with indium standards before measurements. The phase behaviors of the molecules were analyzed using a hot-stage polarized light microscope (Leitz-1350 heating stage coupled with PLM). Cyclic voltammetry measurements were carried out with the model 1100A electrochemical analyzer (CH instruments). It is a conventional three-electrode cell which uses a Pt button working electrode of 2-mm diameter, Pt wire as the counter electrode, and Ag/AgCl as the reference electrode. The measurements were carried out using spectroscopic grade CH_2Cl_2 containing Bu_4NPF_6 (0.1 M) as supporting electrolyte under nitrogen gas protection at a scan rate of 0.1 V/s at 25 °C. All potentials were internally referenced to Fc/Fc^+ couple. The Pt working electrode was polished before each experiment with a 0.05-μm alumina paste, and solutions were purged with nitrogen before starting the measurements.

Synthesis of Amine-Functionalized Perylenebisimides (1a to 1d). *N,N′-bis[12-dodecylamine]perylene-3,4,9,10-tetracarboxyldiimide* (**1b**). A typical synthetic procedure is described for *N,N′*-bis[12-dodecylamine]perylene-3,4,9,10-tetracarboxyldiimide (**1b**). 1,12-Diaminododecane (5.10 g, 25.50 mmol) and zinc acetate (0.001 g, 0.006 mmol) in *N,N*-dimethylacetamide (25 mL) was heated to 110 °C under a nitrogen atmosphere. 3,4,9,10-Perylenetetracarboxylic dianhydride (1.00 g, 2.55 mmol) was added, the reaction mixture was stirred at 110 °C for 3 h, and then the process was continued at 160 °C for 15 h under a nitrogen atmosphere. The excess solvent was distilled off, the slurry was washed several times with hexane, and then it was precipitated into acetone. The reddish-black precipitate was filtered and dried in a vacuum (0.1 mm of Hg) oven for 12 h. It was purified by column chromatography using a chloroform/methanol (70:30 v/v) solvent mixture. Yield: 1.6 g (82%). ^{1}H NMR (300 MHz, $CDCl_3$, TFA) δ ppm: 8.88 (s, 8H, perylene), 4.37 (s, 4H, imide C**H**$_2$), 3.26 (s, 4H, C**H**$_2$ NH$_2$), 1.37−1.83 (m, 40H, C**H**$_2$). FT-IR (KBr, cm^{-1}): 3389, 3296, 3071, 2922, 2850, 1695, 1656, 1593, 1506, 1439, 1403, 1342, 1257, 1155, 1090, 1015, 852, 809, 746, and 630.

A similar procedure was adopted for the synthesis of compounds **1a**, **1c**, and **1d** using 1,6-diaminododecane, 3,8-bis(aminomethyl)-tricyclo[5.2.1.0.(2,6)]decane and 1,3-biscyclohexyl bimethylamine, respectively.

N,N′-Bis[6-hexylamine]perylene-3,4,9,10-tetracarboxyldiimide (**1a**). Yield: 1.3 g (86%). ^{1}H NMR (300 MHz, $CDCl_3$, TFA) δ ppm: 8.84 (s, 8H, perylene), 4.38 (s, 4H, imide C**H**$_2$), 3.27 (s, 4H, C**H**$_2$ NH$_2$), 1.35−1.89 (m, 16H, C**H**$_2$). FT-IR (KBr, cm^{-1}): 3304, 3066, 2937, 2859, 1694, 1631, 1538, 1474, 1367, 1284, 1097, 938, 809, 712, 630, 603, and 505.

N,N′-Bis[3,8-bis(aminomethyl)tricyclo(5.2.1.0.(2,6))decane]-perylene-3,4,9,10-tetracarboxyldiimide (**1c**). Yield: 1.54 g (81.4%). ^{1}H NMR (300 MHz, $CDCl_3$, TFA) δ ppm: 8.89 (s, 8H, perylene), 4.31 (s, 4H, imide C**H**$_2$), 3.38 (s, 4H, C**H**$_2$ NH$_2$), 0.83−2.66 (m, 28H, C**H** and C**H**$_2$ TCD). FT-IR (KBr, cm^{-1}): 3549, 3390, 3291, 3082, 2938, 2916, 1694, 1651, 1593, 1337, 1247, 851, 809, and 745.

N,N′-Bis[1,3-cyclohexylamine]perylene-3,4,9,10-tetracarboxyldiimide (**1d**). Yield: 1.64 g (82%). ^{1}H NMR (300 MHz, $CDCl_3$, TFA) δ ppm: 8.89 (s, 8H, perylene), 4.45 (s, 4H, imide C**H**$_2$), 3.39 (s, 4H, C**H**$_2$ NH$_2$), 1.1−2.3 (m, 20H, C**H** and C**H**$_2$ cyclohexyl). FT-IR (KBr, cm^{-1}): 3391, 3087, 2921, 2851, 1694, 1651, 1594, 1574, 1441, 1399, 1168, 1111, and 809.

Synthesis of Hydroxyl-Functionalized Perylenebisimides (2a and 2e). *N,N′-bis[6-hydroxyhexyl]perylene-3,4,9,10-tetracarboxyldiimide* (**2a**). A typical synthetic procedure is described for *N,N′*-bis[6-hydroxyhexyl]perylene-3,4,9,10-tetracarboxyl diimide (**2a**). 6-Aminohexanol (0.65 g, 5.60 mmol), zinc acetate (0.001 g, 0.006 mmol) in *N,N*-dimethylacetamide (25 mL) was heated to 110 °C under a nitrogen atmosphere. 3,4,9,10-Perylenetetracarboxylic dianhydride (1.00 g, 2.55 mmol) was added, and the reaction mixture was stirred at 110 °C for 3 h and then continued at 160 °C for 15 h under a nitrogen atmosphere. The excess solvent was distilled off, and the slurry was washed several times with hexane and precipitated into acetone. The reddish-black precipitate was filtered and dried in a vacuum (0.1 mm of Hg) oven for 12 h. Yield: 1.3 g (86%). ^{1}H NMR (300 MHz, $CDCl_3$, TFA) δ ppm: 8.85 (s, 8H, perylene), 4.50 (t, 4H, imide C**H**$_2$), 4.35 (t, 4H, C**H**$_2$OH), 1.60−1.89 (m, 16H, C**H**$_2$). FT-IR (KBr, cm^{-1}): 3543, 3516, 2928, 2853, 1690, 1658, 1593, 1443, 1402, 1380, 1345, 1262, 1088, 1036, 978, 856, 809, 748, 631, and 490.

N,N′-Bis[2-hydroxyethyl]perylene-3,4,9,10-tetracarboxyldiimide (**2e**). A similar procedure was adopted for the synthesis of *N,N′*-bis[2-hydroxyethyl]perylene-3,4,9,10-tetracarboxyldiimide (**2e**) using ethanolamine. Yield: 1.02 g (78%). ^{1}H NMR (300 MHz, $CDCl_3$, TFA) δ ppm: 8.83 (s, 8H, perylene), 4.84 (t, 4H, imide C**H**$_2$), 4.77 (t, 4H, C**H**$_2$OH). FT-IR (KBr, cm^{-1}): 3550, 3525, 2939, 2873, 1694, 1653, 1590, 1457, 1412, 1375, 1340, 1087, 989, 856, 819, and 495.

Synthesis of Amide-Functionalized Perylenebisimides (3a−3d). *N,N′-Bis[12-dodecylbenzamide]perylene-3,4,9,10-tetracarboxyldiimide* (**3b**). A typical synthetic procedure is described for *N,N′*-bis[12-dodecylbenzamide]perylene-3,4,9,10-tetracarboxyldiimide (**3b**). **1b** (0.50 g, 0.66 mmol) and pyridine (2.5 mL, 30 mmol) in *N*-methyl pyrollidinone (NMP) (20 mL) was heated to 110 °C under nitrogen to get a homogeneous solution. To this, benzoyl chloride (0.77 mL, 6.60 mmol) was added dropwise over a period of 15 min. The reaction was continued for 12 h and then the excess solvent was removed by distillation under reduced pressure and the slurry was poured into acetone to get a red precipitate. It was filtered and dried in a vacuum (0.1 mm of Hg) oven for 12 h. It was further purified by column chromatography on silica gel using $CHCl_3$/hexane (90:10 v/v). Yield: 0.08 g (13%). ^{1}H NMR (300 MHz, $CDCl_3$) δ ppm: 8.53, 8.36 (dd, 8H, perylene), 7.52−7.12 (m, 10H, benzoyl), 4.19 (t, 4H, imide C**H**$_2$), 4.02 (t, 4H, amide C**H**$_2$), 1.25−1.82 (m, 40H, C**H**$_2$). ^{13}C NMR ($CDCl_3$) δ ppm: 174.1, 162.4 (C═O), 136.8, 133.6, 131.6, 130.7, 128.6, 128.1, 122.9, 122.6, 47.4, 40.6, 31.3, 30.1, 29.6, 29.5, 29.3, 29.2, 28.9, 27.1. FT-IR (KBr, cm^{-1}): 3434, 2923, 2846, 1695, 1655, 1593, 1440, 1343, 1259, 1089, 809, 743, 716, and 691. Anal. Calcd. for $C_{62}H_{68}N_4O_6$: C, 77.15; H, 7.10; N, 5.80. Found: C, 77.56; H, 7.45; N, 5.41. MALDI-TOF MS (MW = 964); m/z = 965.6 $[M + 1]^+$.

A similar procedure was adopted for the synthesis of compounds **3a** and **3c**,**3d** using **1a** and **1c**,**1d**, respectively.

N,N′-Bis[6-hexylbenzamide]perylene-3,4,9,10-tetracarboxyldiimide (**3a**). Yield: 0.22 g (32%). ^{1}H NMR (300 MHz, $CDCl_3$) δ ppm: 8.48−8.33 (dd, 8H, perylene), 7.05−7.5 (m, 10H, benzoyl), 4.12 (t, 4H, imide C**H**$_2$), 3.95 (t, 4H, amide C**H**$_2$), 0.8−1.6 (m, 16H, C**H**$_2$). ^{13}C NMR ($CDCl_3$) δ ppm: 176.2, 167.0 (C═O), 138.8, 135.6, 132.6, 130.6, 129.6, 128.7, 123.9, 122.5, 49.4, 42.6, 36.3, 31.1, 30.6, 29.5, 29.3. FT-IR (KBr, cm^{-1}): 3449, 2925, 2846, 1694, 1654, 1593, 1440, 1403, 1344, 1256, 1073, 809, 746, 694, and 659. Anal. Calcd. for $C_{50}H_{44}N_4O_6$: C, 75.36; H, 5.57; N, 7.03. Found: C, 75.12; H, 5.85; N, 7.21. MALDI-TOF MS (MW = 796); m/z = 797 $[M + 1]^+$

N,N′-Bis[3,8-bis(aminomethyl)tricyclo[5.2.1.0.(2,6)]decanebenzamide]perylene-3,4,9,10-tetracarboxyldiimide (**3c**). Yield: 0.43 g (36%). ^{1}H NMR (300 MHz, $CDCl_3$) δ ppm: 8.43, 8.27 (dd, 8H, perylene), 7.11−7.35 (m, 10H, benzoyl), 3.96−4.11 (8H, imide C**H**$_2$ and amide C**H**$_2$), 0.896−2.09 (m, 28H, C**H** and C**H**$_2$ TCD). ^{13}C NMR ($CDCl_3$) δ ppm: 174.5, 163.4 (C═O), 137.2, 137.1, 131.6, 131.1, 128.7, 128.6, 128.1, 127.9, 123.0, 122.7, 51.6, 44.8, 33.9. FT-IR (KBr, cm^{-1}): 3450, 2945, 2873, 1696, 1655, 1594, 1577, 1434, 1338, 1234, 1020, 809, 716, and 691; MALDI-TOF MS (MW = 952); *m*/*z* = 975.3 [M + Na]$^+$.

N,N′-Bis[1,3-cyclohexylbismethylbenzamide]perylene-3,4,9,-10-tetracarboxyldiimide (**3d**). Yield: 0.13 g (20%). ^{1}H NMR (300 MHz, $CDCl_3$) δ ppm: 8.28, 8.14 (dd, 8H, perylene), 6.69−7.33 (m, 10H, benzoyl), 4.0 (4H, imide C**H**$_2$), 3.82 (4H, amide C**H**$_2$), 1.05−1.92 (m, 20H, C**H**$_2$). ^{13}C NMR ($CDCl_3$) δ ppm: 174.5, 163.4 (C═O), 137.0, 132.7, 131.8, 129.2, 128.6, 128, 126.1, 123.5, 118.9, 53.8, 46.3, 38.0, 36.6, 35.4, 31.1, 30.9, 25.5. FT-IR (KBr, cm^{-1}): 3456, 2923, 2851, 1695, 1656, 1594, 1440, 1403, 1342, 1230, 1074, 809, 745, and 694. MALDI-TOF MS (MW = 849); *m*/*z* = 872 [M + Na]$^+$.

A similar procedure was adopted for the synthesis of compounds **4b**−**4d** using 3,4,5-tridodecyloxybenzoyl chloride with **1b**−**1d**, respectively.

3,4,5-Tridodecyloxybenzoyl Chloride Derivatives (4b−4d). *N,N′-Bis[12-dodecyl-3,4,5-tridodecyloxybenzamide]perylene-3,4,9,10-tetracarboxyldiimide* (**4b**). Yield: 0.20 g (14%). ^{1}H NMR (300 MHz, $CDCl_3$) δ ppm: 7.90−8.0 (d, 8H, perylene), 7.27 (s, 2H, benzoyl), 4.00−4.02 (m, 8H, imide C**H**$_2$ and amide C**H**$_2$), 3.90 (t, 12H, OC**H**$_2$), 0.8−2.1 (m, 178H, C**H**$_2$ and C**H**$_3$). ^{13}C NMR ($CDCl_3$) δ ppm: 167.3, 163.3 (C═O), 153.2, 153.0, 141.2, 134.4, 131.3, 130.2, 129.2, 126.2, 123.9, 108.7, 105.9, 69.6, 69.3, 40.9, 40.4, 32.1, 30.5, 29.9, 29.5, 28.2, 27.3, 27.2, 22.8. FT-IR (KBr, cm^{-1}): 3445, 3280, 2921, 2851, 1693, 1660, 1595, 1574, 1467, 1339, 1226, 1118, 809, 745, and 691.

N,N′-Bis[3,8-tricyclodecane-3,4,5-tridodecyloxybenzamide]-perylene-3,4,9,10-tetracarboxyl diimide (**4c**). Yield: 0.29 g (21%). ^{1}H NMR (300 MHz, $CDCl_3$) δ ppm: 8.0−8.3 (d, 8H, perylene), 7.28 (s, 2H, benzoyl), 4.02−3.91 (m, 8H, imide C**H**$_2$ and amide C**H**$_2$), 3.81 (t, 12H, OC**H**$_2$), 0.9−2.3 (m, 166H, C**H** and C**H**$_2$ TCD; C**H**$_2$ and C**H**$_3$ dodecyl). ^{13}C NMR ($CDCl_3$) δ ppm: 167.3, 163.3 (C═O), 152.2, 152.0, 141.2, 133.4, 131.3, 131.2, 129.2, 127.2, 124.9, 109.7, 105.9, 69.6, 69.3, 40.9, 40.3, 32.3, 30.5, 29.9, 29.6, 28.3, 27.6, 27.3, 23.8. FT-IR (KBr, cm^{-1}): 3391, 2921, 2851, 1694, 1651, 1594, 1574, 1441, 1399, 1342, 1300, 1245, 1168, 1111, 809, and 744.

N,N′-Bis[1,3-cyclohexylbismethyl-3,4,5-tridodecyloxybenzamide]perylene-3,4,9,10-tetracarboxyl diimide (**4d**). Yield: 0.34 g (22%). ^{1}H NMR (300 MHz, $CDCl_3$) δ ppm: 7.97−8.10 (d, 8H, perylene), 7.28 (s, 2H, benzoyl), 4.00−4.03 (m, 8H, imide C**H**$_2$ and amide C**H**$_2$), 3.89 (t, 12H, OC**H**$_2$), 0.9−2.3 (m, 158H, C**H** and C**H**$_2$ cyclohexyl, C**H**$_2$ and C**H**$_3$ dodecyl).^{13}C NMR ($CDCl_3$) δ ppm: 167.3, 163.3, (C═O), 153.2, 152.9, 142.2, 133.7, 131.9, 131.7, 129.2, 127.2, 124.9, 109.7, 105.9, 69.7, 40.9, 40.3, 32.3, 30.5, 28.6, 27.6, 27.3, 23.8. FT-IR (KBr, cm^{-1}): 3445, 3280, 2921, 2851, 1693, 1650, 1595, 1574, 1467, 1339, 1226, 1118, 809, and 746.

Synthesis of Ester-Functionalized Perylenebisimides (5a and 5e). *N,N′-bis[6-hexylbenzoate]perylene-3,4,9,10-tetracarboxyldiimide* (**5a**). A typical synthetic procedure is described for *N,N′*-bis[6-hexylbenzoate]perylene-3,4,9,10-tetracarboxyldiimide (**5a**). **2a** (0.07 g, 0.12 mmol) and pyridine (0.5 mL, 6.00 mmol) in *N*-methyl pyrollidinone (NMP) (20 mL) was heated to 110 °C under nitrogen to get a homogeneous solution. To this, benzoyl chloride (0.03 mL, 0.24 mmol) was added dropwise over a period of 15 min. The reaction was continued for 12 h, then the excess solvent was removed by distillation under reduced pressure, and the slurry was poured into acetone to get a red precipitate. It was filtered and dried in a vacuum (0.1 mm of Hg) oven for 12 h. It was further purified by column chromatography on silica gel using $CHCl_3$/hexane (90:10 v/v). Yield: 0.05 g (75%). ^{1}H NMR (300 MHz, $CDCl_3$, TFA) δ ppm: 8.73 (s, 8H, perylene), 7.33−7.93 (m, 10H, benzoyl), 4.34 (t, 4H, imide C**H**$_2$), 4.21 (t, 4H, ester C**H**$_2$), 1.78, 1.49 (m, 16H, C**H**$_2$). ^{13}C NMR ($CDCl_3$, TFA) δ ppm: 167.1, 163.2 (C═O), 135.6, 134.1, 132.9, 129.8, 129.0, 128.7, 124.2, 122.4, 66.7, 41.5, 28.3, 27.8, 26.6, 25.6. FT-IR (KBr, cm^{-1}): 2931, 2857, 1712, 1693, 1653, 1594, 1439, 1404, 1345, 1272, 1112, 809, 746, 708, and 625. Anal. Calcd. for $C_{50}H_{42}N_2O_8$: C, 75.17; H, 5.30; N, 3.51. Found: C, 75.09; H, 5.17; N, 3.98. MALDI-TOF MS (MW = 798); *m*/*z* = 821.3 [M + Na]$^+$.

N,N′-Bis[2-ethylbenzoate]perylene-3,4,9,10-tetracarboxyldiimide (**5e**). A similar procedure was adopted for the synthesis of *N,N′*-bis[2-ethyl benzoate]perylene-3,4,9,10-tetracarboxyldiimide (**5e**) using **2e**. Yield: 0.20 g (28%). ^{1}H NMR (300 MHz, $CDCl_3$, TFA) δ ppm: 8.88 (s, 8H, perylene), 7.48−7.97 (m, 10H, benzoyl), 4.89 (s, 8H, C**H**$_2$). ^{13}C NMR ($CDCl_3$, TFA) δ ppm: 167.1 (C═O), 135.6, 134.1, 132.9, 129.8, 129.0, 128.7, 124.2, 122.4, 66.7, 41.5, 28.3. FT-IR (KBr, cm^{-1}): 2962, 2857, 1717, 1696, 1658, 1593, 1439, 1402, 1344, 1271, 1177, 1111, 1068, 1025, 809, 745, and 709. Anal. Calcd. for $C_{42}H_{26}N_2O_8$: C, 73.46; H, 3.82; N, 4.08. Found: C, 73.63; H, 3.74; N, 4.27. MALDI-TOF MS (MW = 686); *m*/*z* = 709 [M + Na]$^+$.

Results and Discussion

The synthesis of hydroxyl-, amine-, ester-, and amide-functionalized perylenebisimides was outlined in Scheme 2.We have utilized a stoichiometric controlled polycondensation approach to make the amine-terminated molecules (**1a**−**1d**) using an excess of diamines in the feed.[26] The imidization of perylene-bisanhydride with excess diamine was carried out under two different conditions: using isoquinoline as catalyst in *m*-cresol or zinc acetate as catalyst in *N,N*,-dimethylacetamide (DMAc).[27,28] Though the reaction proceeds well in *m*-cresol, the difficulty in isolation of the product and also the removal of *m*-cresol make the first approach less preferable. On the other hand, DMAc was found to be good; the unreacted diamines and excess solvents were easily distilled out under vacuum, and the crude product was purified by column chromatography. The hydroxyl-functionalized perylenebisimide derivatives (**2a** and **2e**) were synthesized by using twice the equivalents of hydroxyl alkyl amines under the same condition in DMAc. The amides **3a**−**3d** and **4b**−**4d** were prepared by reacting the amine-functionalized perylenebisimide derivatives **1a**−**1d** with benzoyl chloride or 3,4,5-tridodecyloxy benzoyl chloride (gallic acid derivative) in *N*-methylpyrrolidinone/pyridine, respectively. The esters **5a** and **5e** were prepared by reacting **2a** and **2e** with benzoyl chloride similar to their amide counterparts. For easy identification, the samples are also referred to as **Pery-n-x-y**, (see Scheme 2) where n, x, and y represent their spacer (length or type), pendant group (benzoyl or gallic), and chemical linkage (ester or amide), respectively.

The structures of the functionalized perylenebisimides were confirmed by NMR, and the proton NMR spectra of **Pery-12-amine** (**1b**), **Pery-12-Bz-amide** (**3b**), **Pery-12-GA-amide** (**4b**), and **Pery-6-Bz-ester** (**5a**) are given in Figure 1. The various types of protons are labeled by alphabets. In Figure 1a, the imide

SCHEME 2: Synthesis of Perylene-Based Amides and Esters

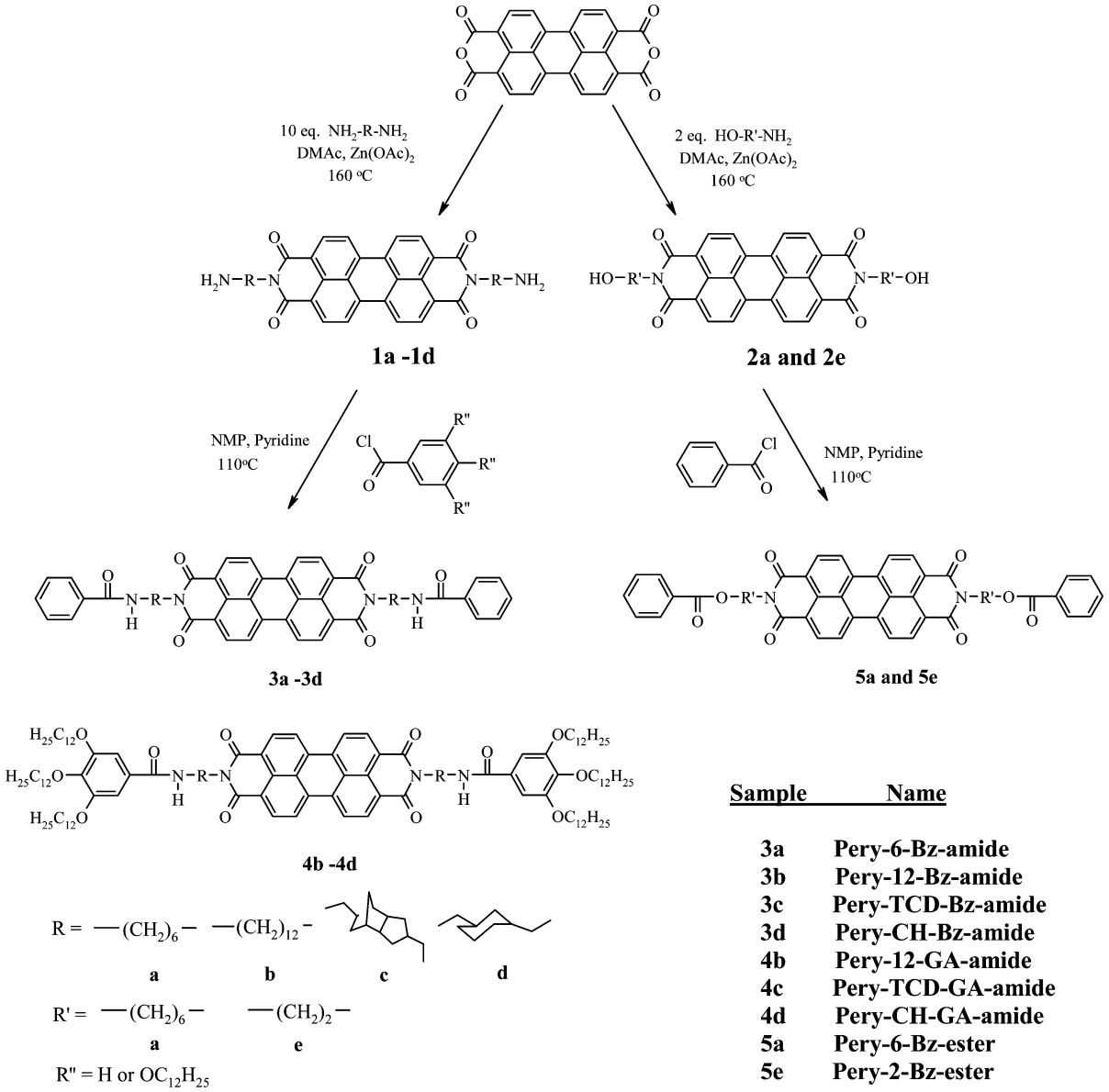

Sample	Name
3a	Pery-6-Bz-amide
3b	Pery-12-Bz-amide
3c	Pery-TCD-Bz-amide
3d	Pery-CH-Bz-amide
4b	Pery-12-GA-amide
4c	Pery-TCD-GA-amide
4d	Pery-CH-GA-amide
5a	Pery-6-Bz-ester
5e	Pery-2-Bz-ester

("a") and $-C\mathbf{H}_2NH_2$ ("b") protons appeared at 4.3 and 3.2 ppm, respectively. Upon the formation of the amide linkages with acid chlorides (in Figure 1, spectra b and c), the methylene amine disappeared completely and a new peak corresponding to the $-C\mathbf{H}_2NHCOPh$ (peak "b′") appeared at 4.0 ppm. The aromatic peaks in the phenyl and gallic ring in Pery-12-Bz-amide (**3b**) and Pery-12-GA-amide (**4b**) appeared with the characteristic splitting patterns with respect to their structures. Similarly, the ^{1}H NMR spectrum of the benzyl ester derivative (Pery-6-Bz-ester, Figure 1d) also matched with expected structures.[29] The intensity of all the peaks exactly matched with the number of protons, which confirms the formation of the expected molecules. The perylenebisimide protons (Pery-H) appeared as a single peak in Figure 1, spectra b and d, whereas two clear doublets appeared in their amide derivative. This is mainly due to the solvent effect since in the presence of trifluoroacetic acid the perylene protons resonate at the same frequency, whereas in $CDCl_3$, as expected, the inner and outer protons differed significantly and appeared as doublets. A high level of purity was achieved for all the compounds by repeated (at least three times) column chromatographic purification until they all showed a single chromatogram in size exclusion chromatography (SEC). The SEC plots of the molecules (see Figure 2) showed a single chromatogram confirming their high purity. As expected, the elution time of the molecules increases with the decrease in the molecular weights (for example, compare Pery-12-GA-amide and Pery-12-Bz-amide). The samples were subsequently subjected to MALDI-TOF analysis, and the mass spectrum of Pery-6-Bz-ester is given in Figure 3. MALDI-TOF mass spectra of the samples were recorded using 2,5-dihyroxy benzoic acid as a matrix, and molecular ion peaks were obtained for either $[M + 1]^+$ or cationic species such as MNa^+, MK^+, and MZn^+.[24] The sodium (also potassium) ions are from the solvents and, interestingly, Zn^+ ions were also picked by the MALDI from trace amounts (ppm level) of the $Zn(OAc)_2$ catalyst left after purification. Thus, the peak at 861.3 in Figure 3 corresponds to the MZn^+ ion, and peaks at the lower mass region, for example, 758.3 and 716.3, correspond to fragments arising from the MZn^+ ion minus the C_6H_5CO radical and the MNa^+ ion minus the C_6H_5CO radical, respectively. The NMR, SEC, and MALDI-TOF mass spectra of molecules confirmed the structure and high purity of the synthesized molecules.

Liquid Crystalline Properties. The thermal stability of the perylene derivatives studied by TGA under a nitrogen atmo-

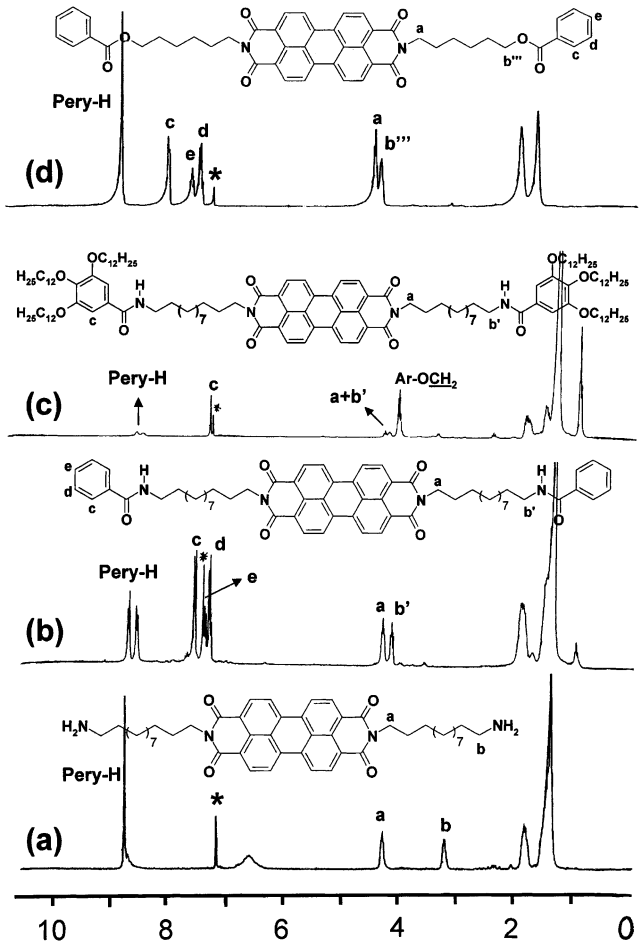

Figure 1. ^{1}H NMR spectra of (a) Pery-12-amine, (b) Pery-12-Bz-amide, (c) Pery-12-GA-amide, and (d) Per-6-Bz-ester (* indicates $CDCl_3$). Spectra a and d are recorded in $CDCl_3/CF_3COOH$, and spectra b and c are recorded in $CDCl_3$.

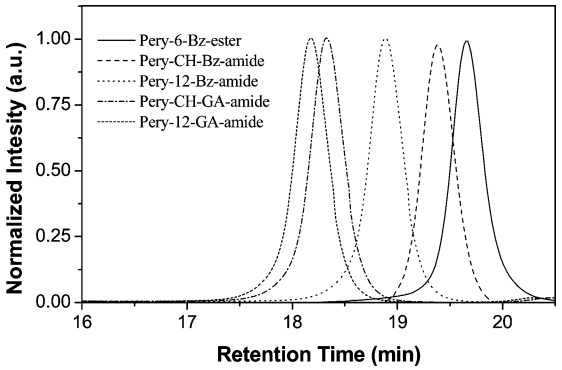

Figure 2. SEC chromatograms of the molecules.

sphere and the 10 wt % loss temperatures for a few of them are summarized in Table 1. All the molecules are stable up to 300 °C, and therefore they can be used for various high-temperature processes in the construction of optoelectronic devices. The thermal properties of the perylenebisimide derivatives were investigated by differential scanning calorimetry (DSC). The heating/cooling DSC thermograms of materials are shown in Figures 4 and 5. Almost all the samples showed multiple transitions in the first heating cycles of their DSC thermograms; however, most of them disappeared during the second heating cycle, indicating that they represented the melting of crystals formed initially by solvent recrystallization.[10] The first heating erases the thermal history of the sample, and the second heating

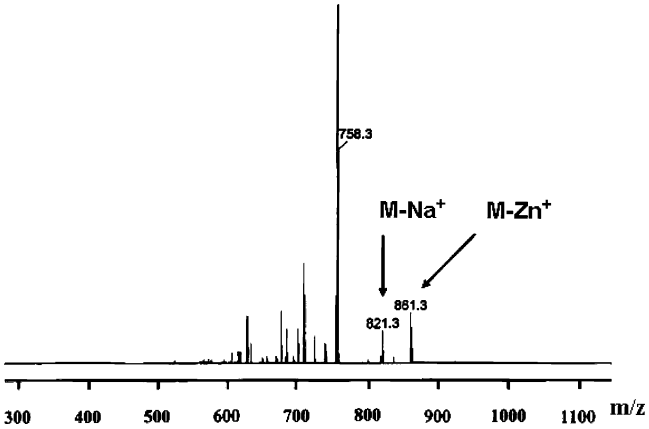

Figure 3. MALDI-TOF spectra of Pery-6-Bz-ester. The peaks at m/z = 758.3 and 716.3 correspond to fragments arising from the MZn^+ ion minus the C_6H_5CO radical and the MNa^+ ion minus the C_6H_5CO radical, respectively.

corresponds to the melting of crystals formed by cooling from the viscous molten phase. Therefore, the data from the second heating cycle and first cooling cycles only are included for discussion here. The DSC trace of Pery-6-Bz-ester (**5a**) showed two transitions upon heating—crystal-to-liquid crystalline and liquid crystalline-to-isotropic at 239 and 258 °C, respectively. While cooling from the melt, two transitions corresponding to the isotropic-to-liquid crystalline (at 222 °C) and liquid crystalline-to-crystal (181 °C) appeared. The liquid crystalline-to-crystal peak in the cooling cycle was quite broad with a shoulder (at 10 °C/min scan rate); however, it appeared as a narrow transition at 174 °C upon very slow cooling (at 2 °C/min, figure not given). Upon reducing the spacer length from C_6 to C_2 (Pery-2-Bz-ester (**5e**)), the liquid crystalline behavior disappeared and 5e did not show any transition in its DSC heating/cooling cycles. The DSC thermograms of Pery-6-Bz-amide (**3a**) showed a clear melting and crystallization peak; however, no phase transition corresponding to the liquid crystalline states were observed. The amine- and hydroxyl-functionalized perylenebisimide derivatives with hexyl spacers (**1a** and **2a**) did not show any transitions in the heating and cooling cycles. Increasing the spacer length in the amide from C_6 to C_{12} in the perylenebisimide induced liquid crystal phases, and Pery-12-Bz-amide (**3b**) showed two transitions in the heating/cooling cycles corresponding to the liquid crystalline behaviors. Surprisingly, the rigid spacer amide counterparts, Pery-CH-Bz-amide (**3d**) and Pery-TCD-Bz-amide (**3c**), did not show any transitions in their heating/cooling cycles. It is well understood in the literature that gallic acid derivatives can induce liquid crystalline phases in the perylenebisimide derivatives. To understand the effect of gallic acid upon induction of the liquid crystalline phase in the current investigation, the DSC thermograms of Pery-12-GA-amide (**4b**), Pery-TCD-GA-amide (**4c**), and Pery-CH-GA-amide (**4d**) were also recorded. Interestingly, Pery-CH-GA-amide (**4d**) showed liquid crystalline behavior and had one transition in the heating scan and one strong transition with a shoulder in the cooling scan. However, the TCD-based gallic acid derivative (Pery-TCD-GA-amide (**4c**)) did not show any melting/crystallization peaks. Pery-12-GA-amide (**4b**) also showed multiple transitions corresponding to crystalline and liquid crystalline phases in the heating scan and two transitions corresponding to isotropic-to-liquid crystalline and liquid crystalline to-crystalline in the cooling scan**.** The detailed DSC analysis clearly demonstrates that the liquid crystalline properties of the perylenebisimide derivatives are highly dependent on the types of the spacers and chemical linkages of the solubilizing pendants.

TABLE 1: Thermal Data for the Novel LC Perylenebisimides

compound	T_m[a] (C−N) (°C)	ΔH_m[a] (C−N) (J/g)	T_m[a] (N−I) (°C)	ΔH_m[a] (N−I) (J/g)	T_c[b] (I−N) (°C)	ΔH_c[b] (I−N) (J/g)	T_c[b] (N−C) (°C)	ΔH_c[b] (N−C) (J/g)	PLM[c] (°C)	T_D[d] (°C)
Pery-6-Bz -ester	239.4	64.43	257.2	1.14	222.7	10.12	180.4	46.25	threadlike	314
Pery-6-Bz -amide	216.3	6.61			189.1	3.92			nil	276
Pery-12-B z-amide	164.7	3.34	206.0	9.50	192.9	5.36			threadlike	262
Pery-12-GA-amide	141.7	3.36	172.7	23.34	144.7	1.31	123.7	6.03	threadlike	396
Pery-CH-GA-amide	209.9	9.45			205.9	5.68			threadlike	404

[a] Measured for the quenched sample in the second heating at 10 °C/min heating rate. [b] Measured for the first cooling cycle from the melt at 10 °C/min cooling rate. [c] Nematic LC phases observed under a polarizing light microscope. [d] Temperature represents 10% weight loss in TGA measurements at a heating rate of 10 °C/min under nitrogen.

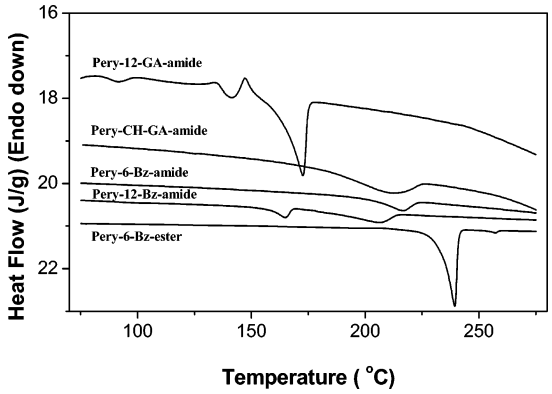

Figure 4. DSC thermograms showing the second heating scans.

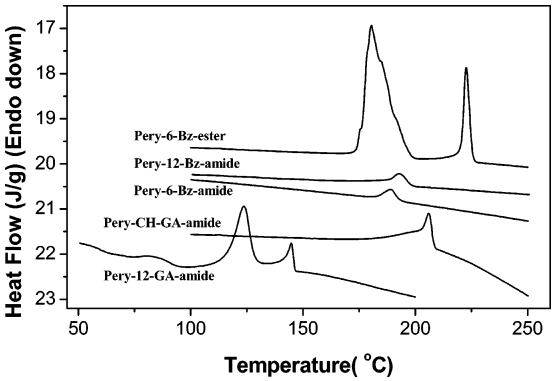

Figure 5. DSC thermograms showing the first cooling scans.

To confirm the liquid crystalline properties, the samples were subjected to polarizing light microscopic (PLM) analysis using a temperature-controlled hot stage. The sample was heated to melt at 10 °C/min and isothermally maintained for 3 min (the melt appeared dark under the polarizer and no crystallites were visible), and the melt was subsequently cooled at 10 °C/min. A threadlike nematic schlieren texture was observed while cooling from the melt and also in the subsequent heating cycle for Pery-6-Bz-ester (**5a**).[30] The liquid crystalline phases of **5a** at various temperatures are shown in the photographs in Figure 6. **5a** was completely melted at 258 °C, and it was held at this temperature for 3 min (Figure 6a). While cooling from the melt, the LC phases started to appear initially which then flowed and started to form a uniform pattern (at 206 °C (Figure 6b)). In the subsequent heating (at 10 °C/min), the LC phases started to re-appear (at 235 °C (Figure 6c)) and they began to flow very gradually (at 251 °C (Figure 6d)). A similar trend was observed for **3b**, and characteristic nematic droplets formed upon cooling from the isotropic phase at 190 °C (Figure 7a); the nematic liquid crystalline phase remained stable even after cooling to room temperature at 30 °C, which suggests that the liquid crystalline phases can be frozen in the polymer matrix for many applications. These results point toward the importance of factors such as the flexibility of the spacer segment and the nature of the linking group in deciding the mesophase nature of the system. Comparing **5a** (Pery-6-Bz-ester) with **3a** (Pery-6-Bz-amide), the core size and spacer length remain the same; however, the linking units in the terminals are different. There are reports in the literature on the liquid crystalline phase inducing behavior of amide versus ester linkage in a cycloaliphatic poly(ester-amide) series.[29] It showed that a small (<10 mol %) percentage of amide linkage introduced into the backbone of a pure cycloaliphatic polyester induced liquid crystalline behavior in the latter. However, >10 mol % of amide units destroyed the liquid crystalline phase, and the pure cycloaliphatic polyamide also was not liquid crystalline. Higher amide content introduces too much rigidity into the system by way of hydrogen bonding, thereby killing the liquid crystal-forming tendency. In the case of Pery-6-Bz-amide (**3a**), also rigidity−flexibility balance is disrupted by the rigid amide linkage. However, upon increasing the length of the flexible spacer segment as in the case of **3b** (Pery-12-Bz-amide), the balance is once again achieved and the system forms a stable nematic liquid crystalline phase, which continues to remain in the liquid crystalline phase even at room temperature upon cooling from the viscous melt. On the other hand, in the case of the cycloaliphatic spacers, **3c** and **3d** are sluggish to crystallize due to high rigidity and fail to produce thermotropic LC phases.

In the gallic amide series, corresponding to the DSC cooling scan, a characteristic nematic threadlike pattern appeared upon cooling from the isotropic melt at 144 °C (Figure 7b) for Pery-12-GA-amide (**4b**). This nematic pattern remained stable up to room temperature (31 °C) as shown in Figure 7c, even though a second transition was observed in the DSC cooling scan at 123 °C. Figure 7d corresponds to the liquid crystalline pattern obtained for **4d** (Pery-CH-GA-amide) upon cooling from the isotropic melt at 204 °C which is very similar to that observed for **4b**. In all the liquid crystalline samples except Pery-6-Bz-ester (**5a**) in the benzoyl and gallic amide series, the liquid crystalline pattern remained stable up to room temperature and disappeared only upon heating. The Pery-TCD-GA-amide (**4c**) did not show any transition in its DSC heating or cooling scan, and no liquid crystalline phase was observed under the microscope. The introduction of the tridodecyloxygallic unit successfully induced liquid crystalline phases in Pery-CH-GA-amide (**4d**), although with a very small window; however, the rigidity of the TCD unit is too high to result in liquid crystalline phases even after introducing the flexible tridodecyloxy groups. A detailed X-ray diffraction analysis (WAXS or SAXS) of perylenebisimides at their liquid crystalline phases would be very useful to get more insight into the three-dimensional solid-state ordering of mesogens.

Electrochemical Properties. Electrochemical properties were investigated by cyclic voltammetry. The measurements were

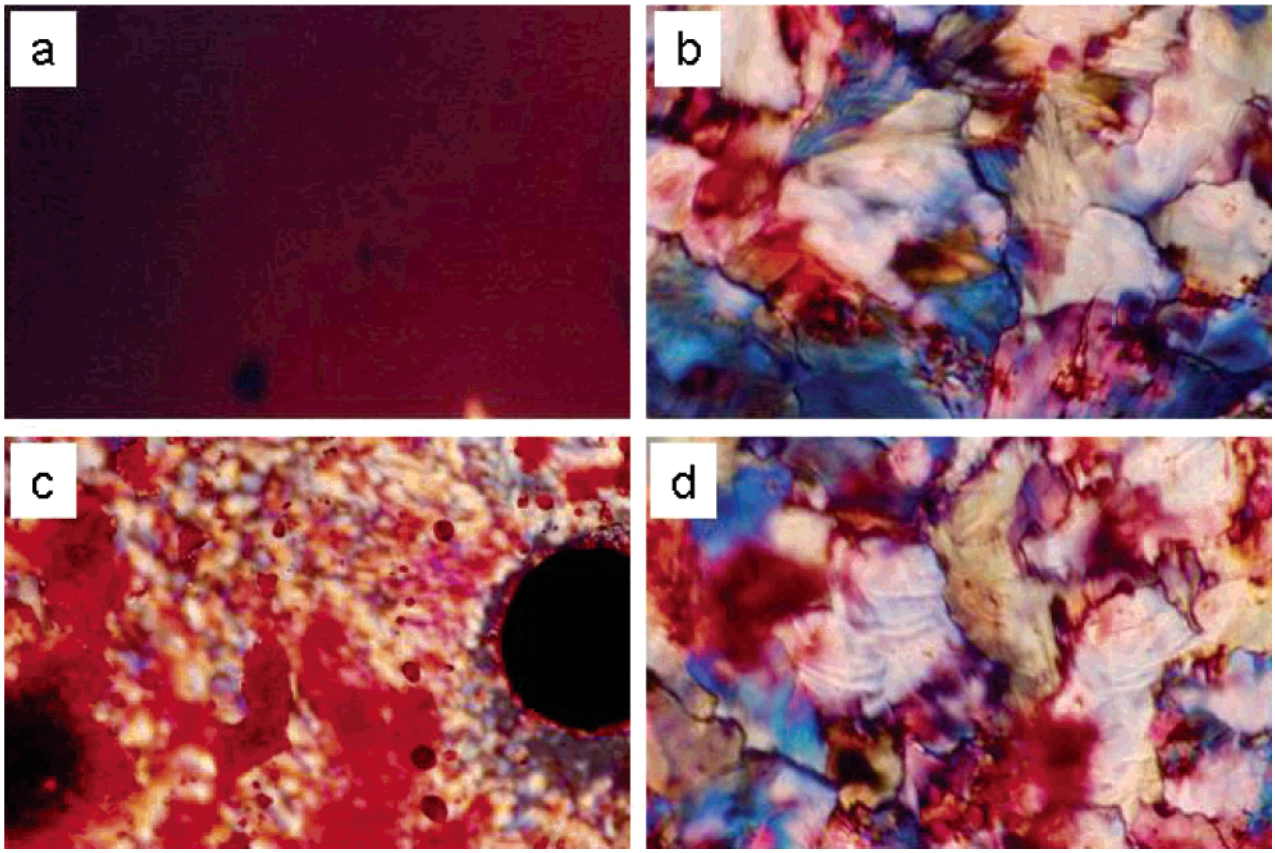

Figure 6. Polarized optical micrographs of the mesophase textures Pery-6-Bz-ester (a) isotropic at 258 °C, (b) nematic schlieren texture at 206 °C upon cooling, (c) nematic pattern starts reappearing at 235 °C upon the second heating, and (d) texture formed fully at 251 °C.

carried out using a platinum electrode in a solution of carefully dried dichloromethane containing 0.1 M tetrabutylammonium hexafluorophosphate ($TBAPF_6$) at room temperature. The potentials were measured against Ag/AgCl as the reference electrode, and each measurement was calibrated with the ferrocene/ferrocenium (Fc) redox system as the internal standard. The voltammograms of a few samples are given in Figure 8. The perylenediimides showed two reversible cathodic currents—the first one about −0.58 to −0.6 V and the second one about −0.76 to −0.80 V vs Ag/AgCl corresponding to the formation of the monoanion and dianion, respectively. These values correspond very well with those reported in the literature.[31−34]All the samples showed only two one-electron peaks corresponding to reduction as is known for perylenediimides. The peak separation value between the two reduction steps, which gives an indication of the extent of twisting of the perylene core, was nearly the same for all these perylenediimides.[34]

Photophysical Properties. The absorption and emission spectra of the perylenebisimides were recorded in chloroform, and a few representative spectra are shown in Figure 9. The absorption spectra for all the molecules were almost identical (except Pery-TCD-Bz-amide (**3c**)) and have characteristic peaks with a maximum at 526 nm and strong vibronic fine structure. The absorption spectrum of Pery-TCD-Bz-amide (**3c**) had a shoulder at 554 nm (shown by an arrow), which could indicate strong molecular aggregation.[24,35] This aggregation peak was also present in other solvents such as THF and toluene. A variable-temperature UV−vis absorption measurement was carried out in toluene for **3c** (Figure 10). The shoulder peak at 554 nm did not disappear at the highest temperature of 90 °C. A 5-nm shift from 531 to 527 nm was observed for all the principal vibronic transitions upon increasing the temperature, and the arrows indicate the hypochromic shift (reduction in intensity) occurring with an increase of temperature. This behavior was perfectly reversible, and the original spectra at 20 °C were recovered after cooling the sample from 90 °C. The decrease in intensity upon heating is due to thermal expansion of the solvent.[36,37] A red-shift of the absorption maximum upon aggregation generally indicates a J-type of aggregate formation.[19,38,39] A variable concentration (range 1×10^{-5} to 1×10^{-6} M) absorption study for Pery-TCD-Bz-amide (**3c**) showed that even at the lowest concentration (1×10^{-6} M) the aggregates were still present. The space-filling models for Pery-TCD-Bz-amide with the other two cyclohexyl and dodecyl counterparts are shown in Figure 11. It is very clear from the figures that the dodecyl and cyclohexyl chains have more free space and are able to undergo free rotation, whereas the TCD system is highly rigid. The increase in the rigidity in the TCD derivative results in an increased hydrogen bonding interaction among the amides, leading to a better π-stacking of the core. To prove the hydrogen bonding interactions, a drop of trifluoroacetic acid was added into the sample in toluene, and the resultant absorbance spectrum is shown in Figure 10 (as a dotted line). The disappearance of the aggregation peak at 554 nm upon addition of trifluoroacetic acid confirmed that it is indeed due to aggregation arising out of strong hydrogen bonding interactions. The bulkiness of the cycloaliphatic ring of TCD hampers a face-to-face packing of chromophores resulting in J-type aggregates. Figure 9 also shows the normalized emission spectra of the perylenebisimide derivatives recorded in chloroform, which have a mirror-image relationship with their respective absorption spectra. The fluorescence spectra of Pery-TCD-Bz-amide (**3c**) was exactly similar to that of the others and did not show any decrease in intensity due to aggregation, indicating that emission originates only from molecularly dissolved species

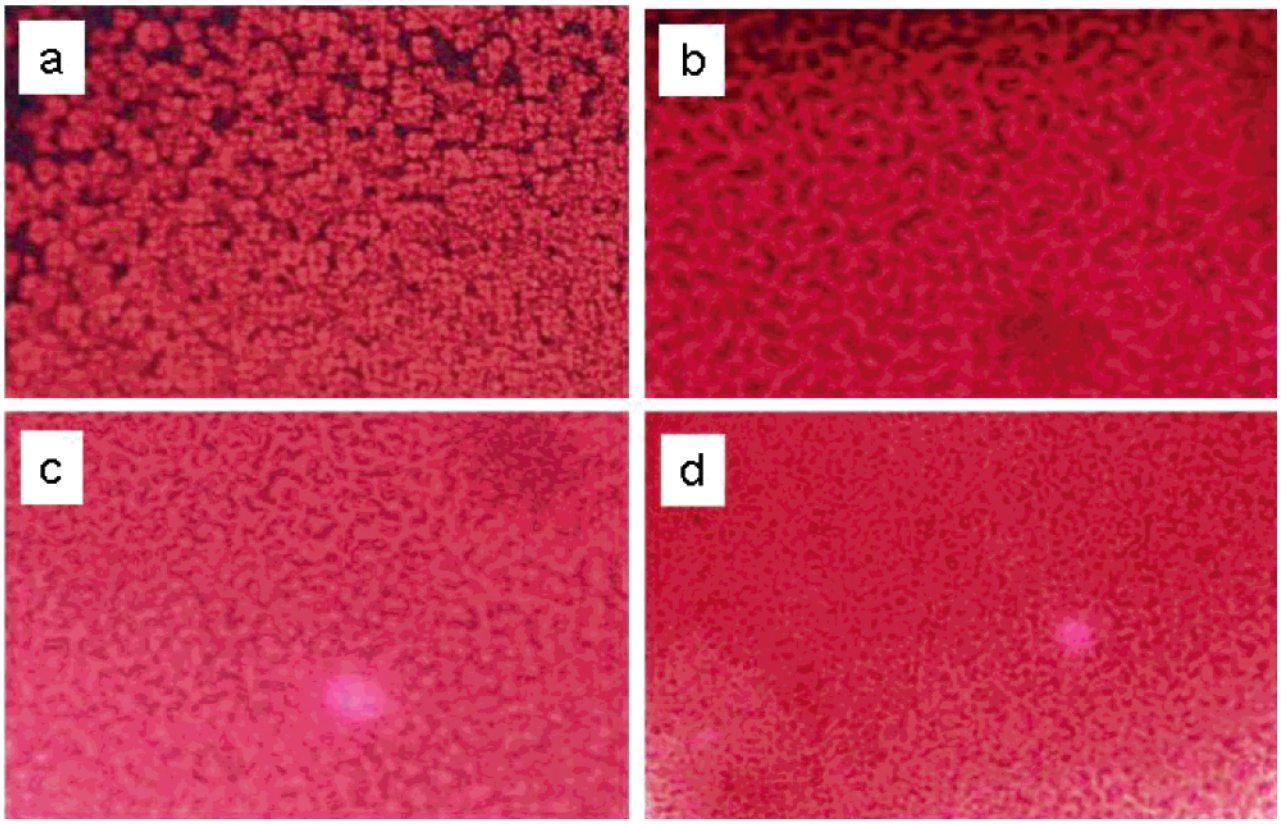

Figure 7. Polarized optical micrographs of (a) Pery-12-Bz-amide: characteristic nematic droplets forming from isotropic melt at 190 °C; (b) Pery-12-GA-amide: nematic threadlike pattern upon cooling from isotropic melt at 144 °C; (c) Pery-12-GA-amide: nematic threadlike pattern remaining stable at RT (31 °C); (d) Pery-CH-GA-amide: nematic threadlike pattern upon cooling from isotropic melt at 204 °C.

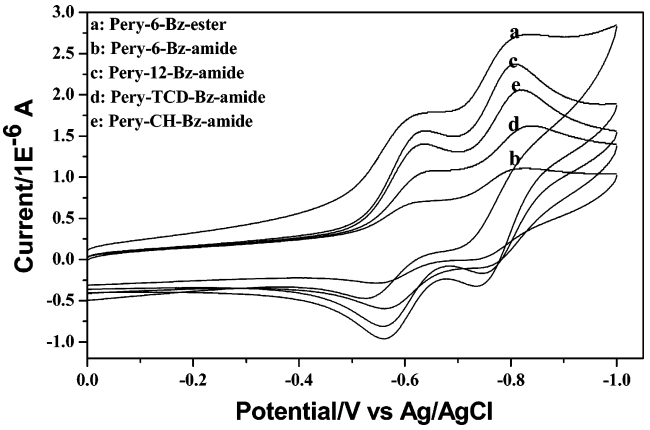

Figure 8. Cyclic voltammograms of perylenebisimide derivatives in 0.1 M Bu_4NPF_6 in dichloromethane, scan rate 0.1 V/s.

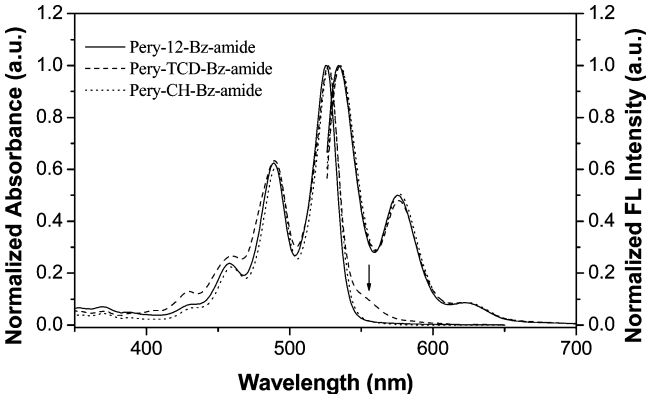

Figure 9. Normalized absorption and fluorescence spectra of the samples in chloroform (dashed line with arrow indicates the aggregation peak of Pery-TCD-Bz-amide).

in solution. The emission quantum yield values were determined in chloroform for all the samples and are given in Table 2.

The quantum yield was measured by a relative method using Rhodamine-6G as the standard in water. The quantum yield was calculated using the following equation:[40]

$$\phi_s = \phi_r(F_sA_r/F_rA_s)(n_r/n_s)^2$$

where ϕ_s is the fluorescence quantum yield, F is the integration of the emission intensities, n is the refractive index of solution, and A is the absorbance of the solution at the exciting wavelength. The subscripts r and s denote reference and sample, respectively. The quantum yield values are much lower than unity and lie in the range of $\phi_s = 0.76-0.81$ for all the samples except for the perylenebisimides with gallic acid derivatives. The quantum yield for the gallic acid series was in the range of 0.01−0.22, and Pery-TCD-GA-amide (**4c**) had the lowest value.

The photoluminescence spectra recorded for thin drop-cast films of the samples showed a remarkable difference in their intensities. Figure 12 gives the combined absorption and photoluminescence spectra of the perylene derivatives drop-cast from $CHCl_3$. For each sample, films of different thickness were prepared by drop-casting from solutions of different concentrations, and films having optical density in the range $< \sim 0.1$ at their λ_{max} were chosen for the photoluminescence measurements. The PL spectra were obtained by exciting at the λ_{max} values, and for each sample the spectra were recorded at different locations to confirm the uniformity of film thickness. The absorption spectra of all the drop-cast film samples were red-shifted as well as broadened compared to their respective solution spectra, indicating aggregation. Additionally, there is

TABLE 2: Photophysical Data of Novel Perylenebisimides

	solution (in $CHCl_3$)			film (on glass plate)		
compound	λ_{max} (abs)	λ_{max}[a] (em)	ϕ_{FL}[b]	λ_{max} (abs)	λ_{max}[a] (em)	PL intensity (10^5)[a] (UV absorbance value)
Pery-2-Bz-ester	526	534	0.80	c		
Pery-6-Bz-ester	526	534	0.77	555	678	6.7 (0.08)
Pery-6-Bz-amide	526	534	0.81	556	680	5.5 (0.07)
Pery-12-Bz-amide	526	534	0.77	551	706	8.6 (0.07)
Pery-CH-Bz-amide	527	534	0.76	553	697	7.7 (0.07)
Pery-TCD-Bz-amide	526	534	0.79	550	681	1.1 (0.09)
Pery-12-GA-amide	525	575	0.22	538	676	3.2 (0.16)
Pery-CH-GA-amide	527	577	0.15	553	665	0.9 (0.10)
Pery-TCD-GA-amide	527	578	0.01	543	669	0.1 (0.15)

[a] Excitation energy is their corresponding absorption maxima. [b] Excitation wavelength is 524 nm for all the compounds; quantum yield calculated using Rhodamine 6G as the standard. [c] Because of solubility problems, film Pery-2-Bz-ester was not formed properly.

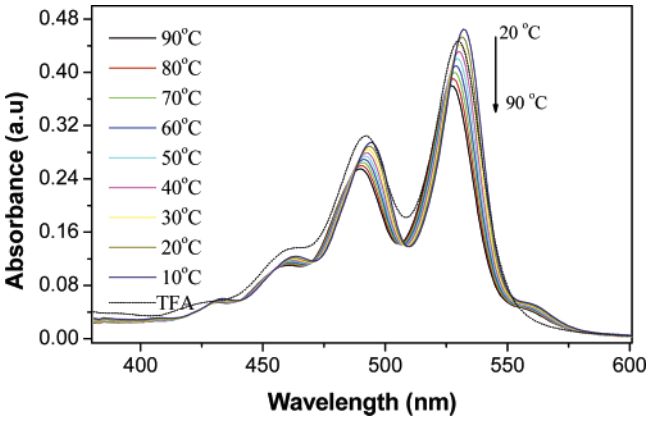

Figure 10. Variable temperature absorption spectra of Pery-TCD-Bz-amide in toluene (1×10^{-5} M) and tolune/TFA (dotted line).

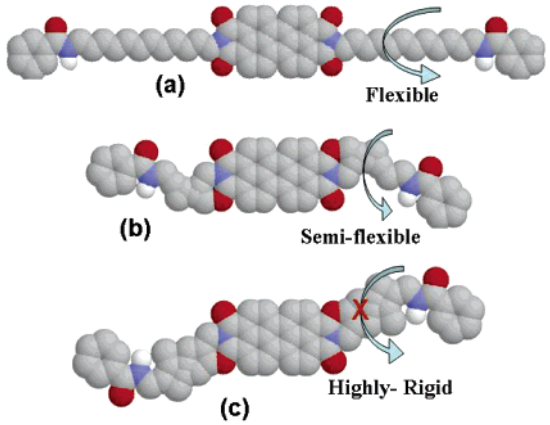

Figure 11. Space filling models for Pery-12-Bz-amide (a), Pery-CH-Bz-amide (b), and Pery-TCD-Bz-amide (c). The arrow indicating the possibility of rotation of the spacer between the perylenebisimide core and the end-capped aryl unit.

also a difference in the ratio of the intensities of the various vibronic transitions. The PL intensity for the molecules is also reported along with their optical density in Table 2. Interestingly, as in the case of the solution, the solid-state luminescence intensity of perylenebisimides with gallic acid derivatives was also quenched severalfold more compared to other samples. The gallic acid unit drastically decreased the luminescence properties of the perylenebisimide core even though it is very good in inducing liquid crystalline phases. In the benzamide series, Pery-TCD-Bz-amide (**3c**) had the lowest PL intensity, which is quenched 5−8-fold more than the others. This is in conformation with the aggregation peak observed in its UV−vis solution spectra and also the space filling model indicating that it is also highly aggregated in the solid state.

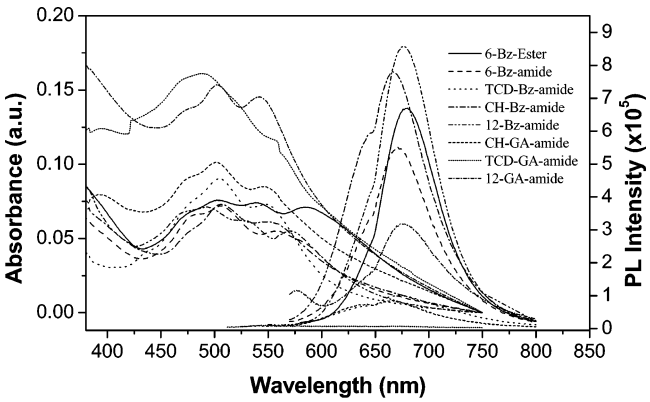

Figure 12. Absorption and photoluminescence spectra of thin films.

In the present investigation, the comparison of PL intensities and quantum yields of both liquid crystalline Pery-12-Bz-amide (**3b**) and Pery-12-GA-amide (**4b**) indicates that the simple phenyl ring is very good for inducing liquid crystallinity without affecting the luminescent properties of the core compared to that of gallic units. The comparison of PL intensities of dodecyl, cyclohexyl, and tricyclodecane spacers in both benzyl and gallic amide series reveals that the linear segment has a higher PL intensity, and it follows the order of dodecyl > cyclohexyl > tricyclodecane. The increase in the rigidity of the spacer decreases the PL intensity of the perylenebisimide core due to an increase of aggregation. Also, comparing the PL intensities of the liquid crystalline samples with their nonliquid crystalline analogues, for example, Pery-6-Bz-ester (**5a**) with Pery-6-Bz-amide (3a), Pery-12-Bz-amide (3b) with Pery-TCD-Bz-amide (**3c**), the former have higher PL intensities for films. Thus, these new perylenebisimides represent a class of highly luminescent LC materials that can retain their characteristics even at room temperature, which makes them desirable as potential candidates for optoelectronic application. Therefore, the present approach clearly demonstrates that LC phases can be induced in perylenebisimide derivatives with suitable choice of spacer segments and connecting linkages without sacrificing their luminescent properties.

Conclusions

The report here attempts a comprehensive study of the various factors such as the spacer length (C_2, C_6, C_{12}), spacer type (linear alkyl vs cycloaliphatic), nature of the linkage (ester, amide, alcohol, amine), or the type of the pendant unit (benzoyl, tridodecyloxygallic) that influences the induction of liquid crystallinity in an important class of conducting perylenebisimides. For the same spacer segment length, the ester linkage was found to be more amenable for liquid crystal formation than the

amidelinkage. However, the highly rigid amide systems also could be made liquid crystalline by increasing the length of the linear alkyl spacer segments. The more rigid cycloaliphatic systems also could be made liquid crystalline by introducing highly flexible tridodecyloxy gallic pendant units. However, though the gallic units are good at inducing liquid crystallinity, they form a poor choice as far as luminescence properties are concerned because they have a tendency to quench the emission. These observations are useful as a design strategy for developing highly luminescent, soluble perylene-based liquid crystalline polymers; work along this direction is currently underway.

Acknowledgment. The authors thank the Department of Science & Technology, New Delhi, India, for funding the work under the Fast Track Scheme for Young Scientists (Project No. SR/FTP/CS-33/2004). We also thank Dr. Suresh Das, RRL-TVM, for the PLM facilities. Thanks are due to CSIR, New Delhi, for a research fellowship to B.J.

Supporting Information Available: MALDI-TOF spectra of the Pery-12-Bz-amide and Pery-TCD-Bz-amide. This material is available free of charge via the Internet at http://pubs.acs.org.

References and Notes

(1) Graser, F.; Hadicke, E. *Liebigs Ann. Chem.* **1980**, 1994−2011.
(2) Popovic, Z. D.; Hor, A. M.; Loutfy, R. O. *Chem. Phys.* **1988**, *127*, 451−457.
(3) Law, K. Y. *Chem. Rev.* **1993**, *93*, 449−486.
(4) Kazmaier, P. M.; Hoffmann, R. *J. Am. Chem. Soc.* **1994**, *116*, 9684−9691.
(5) Tamizhmani, G.; Dodelet, J. P.; Cote, R.; Gravel, D. *Chem. Mater.* **1991**, *3*, 1046−1053.
(6) Bulovic, V.; Burrows, P. E.; Forrest, S. R.; Cronin, J. A.; Thompson, M. E. *Chem. Phys.* **1996**, *210*, 1−12.
(7) Gregg, B. A. *J. Phys. Chem.* **1996**, *100*, 852−859.
(8) Gregg, B. A. *Chem. Phys. Lett.* **1996**, *258*, 376−380.
(9) Cormier, R. A.; Gregg, B. A. *J. Phys. Chem. B* **1997**, *101*, 11004−11006.
(10) Cormier, R. A.; Gregg, B. A. *Chem. Mater.* **1998**, *10*, 1309−1319.
(11) Schlichting, P.; Rohr, U.; Müllen, K. *J. Mater. Chem.* **1998**, *8*, 2651−2655.
(12) Pressner, D.; Goltner, C.; Spiess, H. W.; Müllen, K. *Acta Polym.* **1994**, *45*, 188−195.
(13) Göltner, C.; Pressner, D.; Müllen, K.; Spiess, H. W. *Angew. Chem., Int. Ed. Engl.* **1993**, *32*, 1660−1662.
(14) Müller, G. R. J.; Meiners, C.; Enkelmann, V.; Geerts, Y.; Müllen, K. *J. Mater. Chem.* **1998**, *8*, 61−64.
(15) Rohr, U.; Schlichting, P.; Bohm, A.; Gross, M.; Meerholz, K.; Braüchle, C.; Müllen, K. *Angew. Chem., Int. Ed. Engl.* **1998**, *37*, 1434−1437.
(16) Struijk, C. W.; Sieval, A. B.; Dakhorst, J. E. J.; van Dijk, M.; Kimkes, P.; Koehorst, R. B. M.; Donker, H.; Schaafsma, T. J.; Picken, S. J.; van de Craats, A. M.; Warman, J. M.; Zuilhof, H.; Sudhölter, E. J. R. *J. Am. Chem. Soc.* **2000**, *122*, 11057−11066.
(17) vanHerrikhuyzen, J.; Asha, S. K.; Schenning, A. P. H. J.; Meijer, E. W. *J. Am. Chem. Soc.* **2004**, *126*, 10021−10027.
(18) Leroy, S.; Perrin, L. L.; Baffreau, J.; Hudhomme, P. *Comptes Rendus Chim.* **2006**, *9*, 240−246.
(19) Würthner, F.; Thalacker, C.; Diele, S.; Tschierske, C. *Chem. Eur. J.* **2001**, *7*, 2245−2253.
(20) Würthner, F. *Chem. Commun.* **2004**, 1564−1579.
(21) Leroy-Lhez, S.; Baffreau, J.; Perrin, L.; Levillain, E.; Allain, M.; Blesa, M.; Hudhomme, P. *J. Org. Chem.* **2005**, *70*, 6313−6320.
(22) Chen, Z.; Debije, M. G.; Debaerdemaeker, T.; Osswald, P.; Würthner, F. *ChemPhysChem* **2004**, *5*, 137−140.
(23) Würthner, F.; Sautter, A.; Thalacker, C. *Angew. Chem., Int. Ed.* **2000**, *39*, 1243−1245.
(24) Asha, S. K.; Schennig, A. P. H. J.; Meijer, E. W. *Chem. Eur. J.* **2002**, *8*, 3353−3360.
(25) Peeters, E.; van Hal, P. A.; Meskers, S. C. J.; Janssen, R. A. J.; Meijer, E. W. *Chem. Eur. J.* **2002**, *8*, 4470−4474.
(26) Odian, G. *Principles of Polymerization*, 3rd ed.; John Wiley and Sons: NewYork, 1991; 79 pp.
(27) Lee, C.; Joo, S.; Kim, O.; Ko, J.; Gong, M. *Dyes Pigments* **2002**, *52*, 37−45.
(28) Mackinnon, S. M.; Wang, Z. Y. *J. Polym. Sci., Part A: Polym. Chem.* **2000**, *38*, 3467−3475.
(29) Deepa, P.; Divya, K.; Jayakannan, M. *J. Polym. Sci., Part A: Polym. Chem.* **2006**, *44*, 42−52.
(30) Cojocariu, C.; Rochon, P. *Macromolecules* **2005**, *38*, 9526−9538.
(31) Gomez, R.; Segura, J. I.; Martin, N. *Org. Lett.* **2005**, *7*, 717−720.
(32) Chen, S.; Liu, Y.; Qiu, W.; Sun, X.; Ma, Y.; Zhu, D. *Chem. Mater.* **2005**, *17*, 2208−2215.
(33) Gregg, B. A.; Cormier, R. A. *J. Phys. Chem. B* **1998**, *102*, 9952−9957.
(34) Posch, P.; Thelakkat, M.; Schmidt, H. W. *Synth. Met.* **1999**, *102*, 1110−1112.
(35) Schouwink, P.; Schafer, A. H.; Seidel, C.; Fuchs, H. *Thin Solid Films* **2000,** *372*, 163−168.
(36) Neuteboom, E. E.; Janssen, R. A. J.; Meijer, E. W. *Synth. Met.* **2001**, *121*, 1283−1284.
(37) Neuteboom, E. E.; Hal, P. A. V.; Janssen, R. A. J. *Chem. Eur. J.* **2004**, *10*, 3907−3918.
(38) Kasha, M. *Radiat. Res.* **1963**, *20*, 55−70.
(39) Beckers, E. H. A.; Meskers, S. C. J.; Schenning, A. P. H. J.; Chen, Z.; Würthner, F.; Marsal, P.; Beljonne, D.; Cornil, J.; Janssen, R. A. J. *J. Am. Chem. Soc.* **2006**, *128*, 649−657.
(40) Feng, L.; Chen, Z. *Polymer* **2005**, *46*, 3952−3956.